Supporting information for the manuscript:

A thiamine-dependent enzyme utilizes an active tetrahedral intermediate in vitamin K biosynthesis

Haigang Song , [†,‡,∥] Chen Dong,[†,⊥] Mingming Qin,[†,‡] Yaozong Chen,[†,‡] Yueru Sun,[†,‡,⊤] Jingjing Liu,[§] Wan Chan,[†,§] Zhihong Guo*[†,‡]

[†]Department of Chemistry, [‡]State Key Laboratory for Molecular Neuroscience, [§]Environmental Science Program, The Hong Kong University of Science and Technology, Clear Water Bay, Kowloon, Hong Kong SAR, China.

This file includes:

Materials and Methods

Materials. Thiamine diphosphate (ThDP), NAD^+, pyruvate, α-ketoglutaric acid, magnesium chloride, manganese (II) sulfate, 1-thio-β-D-galactopyranoside, salts, PEG 3350, PEG MME 5000, glycerol and buffers were purchased from Sigma−Aldrich. Restriction enzymes and T4 DNA ligase were purchased from New England Biolabs. UV−vis absorbance was measured using a UV-1800 spectrophotometer from Shimadzu Corporation. PCR amplification and site-directed mutagenesis were conducted with a PTC-200 Peltier thermal cycler from MJ Research. Protein chromatography was done using an ÄKTA Protein Purification System from GE Healthcare Life Sciences. HPLC analysis and purification were carried out using a Waters 600E system with model 2487 dual λ absorbance detector. ^{1}H-NMR experiments were performed using a Bruker AVIII 400 NMR spectrometer. Primers were ordered from Life Technologies and DNA sequencing was done by BGI. PyMol was used to generate all the structure graphics.[1]

Expression and purification of MenD. The gene of *E. coli menD* was amplified from pETM-MenD[2] and subcloned into pET28a(+) between *NcoI* and *XhoI* restriction site for expression as an untagged protein with two extra residues (Met-Ser) at the N-terminus. The primers used in this gene amplification were CCCGCCATGGCAATGTCAGTAAGCGCAT TTAA (*menD* forward) and CCGCCTCGAGTCATAAATGGCTTACACTCG (*menD* reverse). The recombinant plasmid was introduced into BL21 (DE3) for growth in LB medium supplemented with 50 μg/ml kanamycin at 37 °C. The protein was expressed at 18 °C for 18 h by addition of 0.1 mM IPTG when OD_{600} reached 0.8. The wild-type MenD protein was first precipitated from the crude extract with 40% saturated ammonium sulfate (about 1.57 M) and then re-dissolved in 12 ml of 25 mM Tris-HCl (pH 8.0) buffer containing 10% glycerol. After salt removal with a HiPrep 26/10 Desalting column (GE Healthcare), the protein solution was loaded on to a HiPrep DEAE FF 16/10 column (GE Healthcare) for purification with a linear gradient of 100% buffer A (25 mM Tris-HCl (pH 8.0) solution containing 10% glycerol) to 100% buffer B (25 mM Tris-HCl (pH 8.0) solution containing 1 M NaCl and 10% glycerol). The MenD-containing fractions were collected at 10-12% of buffer B, concentrated and loaded to a HiPrep Sephacryl S-200 column for further purification to near homogeneity with a purity > 95% as estimated from an SDS−PAGE gel. The purified MenD solution was concentrated to 58 mg/ml and stored in 25 mM Tris-HCl (pH 8.0) buffer containing 10% glycerol at -20 °C. In a typical purification, 240 mg MenD was obtained from 3 L shake-flask culture.

Activity tests. The isochorismate substrate was prepared from EntC and chorismic acid, as described previously and purified using the reported methods with minor modification.[2-4] Typically, 4 mg chorismic acid was incubated with 10 μM EntC in 500 μl of 50 mM Tris-HCl (pH 8.0) buffer solution containing 50 mM NaCl and 2 mM $MgCl_2$ for 2 h at 37 °C. Isochorismate was then loaded to an Xterra semipreparative C-18 reversed-phase column (10

μm, 7.8 × 300 mm) and eluted with a linear gradient from 100% of buffer A (water containing 1% formic acid) to 100% of buffer B (acetonitrile containing 1% formic acid) over 45 min at a flow rate of 2.0 ml/min after 10 min washing with 100% buffer A on the Waters 600 HPLC system. Isochorismate-containing fractions with a retention time of 25.4 min were collected, lyophilized and frozen at -80 °C. In enzymatic assays, isochorismic acid was freshly dissolved in pure water and its concentration was determined by absorbance at 278 nm ($\varepsilon = 8300\ M^{-1}\cdot cm^{-1}$).[2] After purification, MenD was assayed to have a specific activity consistent with the reported value using a spectroscopic method monitoring isochorismate consumption at 278 nm.[2] Mg^{2+} was found to be completely replaceable with Mn^{2+} at the same concentration in this assay without reducing the MenD activity. In other MenD activity tests, the SEPHCHC product was further converted to SHCHC for UV-vis detection at 290 nm using MenH as the coupling enzyme.[5, 6]

In a typical single turnover experiment, the post-decarboxylation intermediate was formed by adding 25 μM α-ketoglutaric acid to a solution containing 50 μM MenD, 5 μM MenH, 100 μM ThDP and 2 mM $MgSO_4$ in 400 μl of 100 mM potassium phosphate buffer (pH 7.0). Under these conditions, the intermediate was formed almost instantly as monitored by circular dichroism spectroscopy. After mixing, the second substrate isochorismate was added to a final concentration of 60 μM at different reaction time points and the reaction was subsequently quenched after 10 min by adding 100 μl of 2 M CF_3COOH. MenH at the given concentration was tested to be capable of converting all SEPHCHC to SHCHC within a short period of time (< 1 min) at room temperature. After removal of the precipitated protein by centrifugation, 390 μl of the reaction mixture was mixed with 10 μl of 5.3 mM NAD^+ (internal standard) and the SHCHC product was then subjected to HPLC quantification after isocratic elution with an aqueous solution containing 1% formic acid on an analytical C-18 reversed-phase column. The control reaction was performed by simultaneous addition of the ketoacid and isochorismate substrates to the enzyme solution and quenched after 10 min incubation at room temperature.

SHCHC was chemoenzymatically synthesized as a standard in the HPLC analysis using a described method.[5, 6] In a typical preparation, 4 mg chorismic acid was incubated with 10 μM EntC, 25 μM MenD and 10 μM MenH in 500 μl of 200 mM potassium phosphate buffer (pH 7.4) containing 50 mM α-ketoglutaric acid, 80 μM ThDP and 7.5 mM $MgSO_4$ at 37 °C for 3 h. After removal of enzymes by ultrafiltration, SHCHC was eluted isocratically with an aqueous solution containing 1% formic acid at a flow rate of 2 ml/min on the Waters 600 HPLC system using an Xterra semipreparative C-18 reversed-phase column (10 μm, 7.8 × 300 mm). The peak fractions containing SHCHC were collected, lyophilized and frozen at -80 °C.

Circular dichroism (CD) analysis of the intermediate formation. Static spectra were recorded on a JASCO J-815-150S CD spectrometer in a 10 mm path length cell in the near-UV (270–370 nm) wavelength region at a bandwidth of 2 nm. In a typical experiment, α-ketoglutaric acid (final concentration: 2 mM) was added to a 100 mM potassium phosphate

buffer solution (pH 7.0) containing 2.2 mg/ml (33 μM) MenD, 200 μM ThDP and 2 mM $MgSO_4$ and the mixture was immediately analyzed by the CD spectroscopy. The CD spectra were taken every 5 min and were not found to significantly change over a period of 30 min at room temperature. Control CD spectra were taken in the absence of α-ketoglutaric acid with or without ThDP. The ThDP-bound intermediate gave rise to a species with a positive signal at 301 nm and a broad intense negative signal from 307-365 nm with double minima at 320 nm and 330 nm, which are absent in the enzyme with or without the ThDP cofactor. These observed spectral features are clearly different from those of the enamine intermediate in transketolase, which shows positive circular dichroism signals in the ranges of 290-295 nm and >300 nm (Fiedler et al. *Proc. Natl. Acad. Sci. USA* **2002,** *99*, 591.).

To determine what is formed in the reaction of α-ketoglutaric acid with MenD, the reaction (with the scale as in the CD experiment) was carried out and quenched immediately with trifluoroacetic acid 20 seconds after addition of the keto-acid substrate at room temperature. After removal of the precipitated protein, the reaction mixture was analyzed by ESI-MS with a spectrum as shown in Fig. S5(A). Only the succinic semialdehyde-ThDP adduct (see below) and free ThDP were detected in the mixture, while the predecarboxylation ThDP adduct (molecular formula: $C_{17}H_{25}N_4O_{12}P_2S^+$; calculated molecular weight: 571.07) was never detected.

Deuterium exchange of the $C_{2\alpha}$-associated proton of the intermediate. To examine the exchangeability of the $C_{2\alpha}$-associated proton, the postdecarboxylation intermediate was first prepared by incubating 500 μM MenD with 500 μM α-ketoglutaric acid, 500 μM ThDP and 5 mM $MgSO_4$ in 2 ml of 100 mM phosphate buffer (pH 7.0) solution. After 5 min reaction at room temperature, an equal volume of D_2O was added to the reaction mixture and the resulting solution was further incubated for 30 min at room temperature to allow deuterium exchange before the reaction was quenched by addition of 1 ml of 2 M CF_3COOH. After removal of the precipitated protein by centrifugation, the reaction mixture was concentrated by lyophilization and re-dissolved in a minimum amount of pure water. The succinic semialdehyde-ThDP adduct with a retention time of 6.2 min was then purified by HPLC from the reaction mixture using an Xterra semi-preparative C-18 reversed-phase column (10 μm, 7.8 × 300 mm) and isocratic elution with water containing 1% formic acid at a flow rate of 2 ml/min. A small volume of the eluted fraction was taken out for ESI-MS analysis and the remaining portion was lyophilized and further re-dissolved in 200 μl D_2O for ^{1}H-NMR experiment. As a control, the reaction was carried out using an equal volume of H_2O instead of D_2O in the exchange experiment and the non-deuterated ThDP adduct was purified and analyzed in parallel. It was found that a significant amount of glycerol ended up in the purified ThDP adduct to interfere with the ^{1}H-NMR analysis when MenD was purified and stored in buffers containing 10% glycerol. To reduce this interference, MenD in the deuterium exchange experiments was purified freshly in glycerol-free buffers and used directly in the reactions. MenD freshly purified in the absence

of glycerol was found to have the same activity as the enzyme stored in 10% glycerol in enzymatic assays.

In the mass spectrum of the isolated succinyl semialdehyde-ThDP, two molecular ions were detected at m/z = 527 (M) and 528 (M+1). Assuming that the intensity ratio of the (M+1): M is R_H and R_D before and after the exchange, respectively, the rate of deuterium incorporation is equal to $(R_D-R_H)/(1-R_H)$. This deuterium incorporation rate was also calculated from the decrease in the normalized intensity of C2α-H relative to C6'-H in ^{1}H-NMR spectrum of the isolated product from the deuterium exchange experiment.

Crystallization of MenD and soaking with the substrates. Initial screening of the crystallization conditions for the wild-type MenD was performed in the presence of ThDP and Mn^{2+} with the hanging-drop diffusion method at 289K using commercially available screening kits, including Index Screen, PEG/Ion screen, Crystal Screen I and II from Hampton Research and Wizard Screen I and II from Rigaku Corporation. Subsequent optimization of the preliminary conditions led to plate-like crystals within 4 days with desirable diffraction qualities by mixing 1 μl protein solution (5 mg/ml protein supplemented with 0.5 mM ThDP and 5 mM $MnSO_4$) with 1 μl reservoir condition (0.16 M magnesium formate, 1% Tascimate pH 7.0, 0.02 M HEPES pH 7.0, 14% PEG 3350 and 2% PEG MME 5000). These crystals were used in the soaking experiments (see below) to obtain most crystal structures shown in Table S1 (all but PDB ID: 5EJ8). Under the same conditions, crystals were found to continue to grow and form bigger single crystals with better diffraction quality and resolution after three months at 16 °C. These later crystals were used to obtain the structure at 1.34 Å resolution (PDB ID: 5EJ8). In these experiments, addition of 5 mM $MnSO_4$ was found to be crucial to the growth and diffraction quality of the resulting crystals. As a result, Mn^{2+} was modeled as the metal ligand of the pyrophosphate moiety of the ThDP cofactor in the resulting structures despite the fact that the crystals were grown in the presence of magnesium ion at a much higher concentration.

In the soaking experiments, the grown single crystals were soaked in the cryo-protecting solution containing the ketoacid substrate (the mother liquor supplemented with 20% glycerol and 10 mM α-ketoglutarate) for a time period ranging from 21 s to 1.5 h. At different time points, the soaking reactions were stopped by directly transferring the crystals into liquid nitrogen for data collection.

To test the activity of the post-decarboxylation intermediate, the MenD single crystals were first soaked in 10 mM α-ketoglutarate for 2 min to form the postdecarboxylation intermediate as described above. Subsequently, the resulting crystals were transferred into the mother liquor supplemented with 20% glycerol to remove the extra α-ketoglutarate and then transferred into another cryo-protecting solution comprising of the mother liquor supplemented with 20% glycerol and 250 μM isochorismate for a time period up to 20 min without damaging the crystals. At different time points, the crystals soaked with isochorismate were transferred to

liquid nitrogen and frozen for data collection. The SEPHCHC product in the mother liquid was converted to SHCHC for UV-vis detection at 290 nm using MenH as the coupling enzyme.[5, 6] In the second soaking experiment, the MenD crystals cracked immediately when isochorismate concentration was 500 μM.

Data collection, structural determination and refinement. All the X-ray data were collected at BL17U beamline of the Shanghai Synchrotron Radiation Facility (SSRF) with an ADSC Quantum 315R charge-coupled device detector or BL19U of the National Center for Protein Science Shanghai (NCPSS) with a PILATUS3 6M detector at 100 K. For the 1.34-Å-resolution structure, the data were collected at different spots of the crystal to minimize radiation damage. Diffraction images were either processed with HKL2000[7] or indexed, integrated with iMosfilm[8] and scaled with Aimless.[9] All the structures were solved by molecular replacement with Phaser[10] using *E. coli* MenD (PDB entry 2JLC)[11] as initial search model. The generated model was further manually built by COOT[12] and refined by PHENIX.[13] TLS and NCS were used in the refinement of all crystal structures. For the higher resolution structure at 1.34 Å resolution (PDB ID: 5EJ8), a slightly different refinement procedure was followed with water molecules added at 1.5 Å resolution and re-checked at 1.34 Å resolution. Hydrogen atoms of the residues were automatically generated using the riding model in PHENIX at 1.34 Å resolution. TLS and NCS refinement methods were used in the middle refinement cycles. Anisotropic atomic displacement parameter refinement for all the non-hydrogen atoms was applied in the final several refinement cycles. The restraints for the ligands were generated using PRODUG[14] and optimized by eLBOW.[15] The overall qualities of all the finalized structures were assessed by PROCHECK[16] and MolProbity.[17] The data statistics for collection and refinement of the structures are summarized in Table S1 with Ser391 as a Ramanchandran outlier as in other known MenD structures (PDB entries 2JLA, 2JLC, and 2X7J).

Table S1. Data collection and refinement statistics

	MenD-KG-2 min	MenD-KG-21 s	MenD-KG-15 min	MenD-KG-1.5 h	MenD-KG-2 min-Iso-2 min	MenD-KG-2 min-Iso-7min	MenD-KG-2 min-Iso-13 min
PDB ID	**5EJ8**	**5EJ7**	**5EJ4**	**5EJ5**	**5EJ6**	**5EJA**	**5EJ9**
Space group	P_1	P_1	P_1	P_1	P_1	P_1	P_1
***a*, *b*, *c* (Å)**	90.66, 90.76, 169.34	90.60, 90.61, 167.57	90.79, 90.77, 169.56	90.76, 90.80, 170.10	90.48, 90.51, 171.64	90.61, 90.66, 169.46	90.72, 90.72,169.47
α, β, γ (°)	83.25, 76.03, 64.32	76.08, 83.45, 63.44	83.27, 76.01, 64.30	75.79, 83.29, 64.34	83.02, 75.85, 64.33	76.03, 83.39, 64.41	76.06, 83.35, 64.38
Reflection	2345165 (1002427)	1250745 (634680)	874242 (443335)	371017 (194725)	544093 (213686)	1146914 (583261)	962167 (487194)
Redundancy	2.3 (2.4)	2.0 (2.0)	2.0 (2.0)	1.9 (1.9)	2.5 (2.4)	2.0 (2.0)	2.0 (2.0)
Completeness (%)	94.5 (92.4)	96.0 (91.3)	96.6 (94.8)	92.4 (95.5)	93.7 (82.7)	93.6 (93.4)	96.5 (91.2)
$I/\sigma(I)$	5.0 (2.0)	6.4 (3.5)	7.1 (2.5)	5.8 (2.8)	6.7 (3.9)	6.9 (2.4)	8.1 (3.1)
R_{merge}[a]	0.123 (0.409)	0.063 (0.192)	0.077 (0.417)	0.101 (0.240)	0.120 (0.213)	0.070 (0.303)	0.048 (0.156)
Refinement							
Resolution (Å)	27.65–1.34	33.49–1.56	41.82–1.77	36.28–2.30	34.89–2.24	50.52–1.60	41.85–1.72
R_{work} / R_{free}[b]	0.1328/0.1636	0.1458/0.1830	0.1758/0.2169	0.1830/0.2343	0.1951/0.2414	0.1697/0.1934	0.1507/0.1820
No. of atoms							
Overall	41700	42006	39500	36620	36629	40595	40439
Protein	35426	35538	34751	34668	34508	34826	34712
Ligands	598	357	392	320	272	320	330
Water	5676	6111	4357	1632	1849	5449	5397
RMS (bonds) (Å)	0.008	0.006	0.007	0.008	0.008	0.008	0.007
RMS (angles) (°)	1.070	1.062	1.076	1.150	1.156	0.972	1.070
Ramachandran plot							
Favored (%)	97.81	97.69	98.14	98.00	97.95	97.70	97.96
Allowed (%)	2.01	1.20	1.73	1.98	2.03	2.14	1.86
Outliers (%)	0.18	0.11	0.13	0.02	0.02	0.16	0.18
Average *B*-factor (Å^2)							
Overall	17.4	17.1	19.1	26.0	17.0	17.7	19.3
Protein	15.2	14.8	17.9	25.8	16.8	15.5	17.4
Ligands	20.1	15.2	21.1	27.7	15.7	21.5	19.3
Solvent	30.9	30.6	29.1	29.9	21.6	31.5	31.5

a. $R_{merge} = \Sigma|I_i - I_m|/\Sigma I_i$, where I_i is the intensity of the measured reflection and I_m is the mean intensity of all symmetry related reflections.

b. $R_{work} = \Sigma||F_{obs}| - |F_{calc}||/\Sigma|F_{obs}|$, where F_{obs} and F_{calc} are observed and calculated structure factors. $R_{free} = \Sigma T||F_{obs}| - |F_{calc}||/\Sigma T|F_{obs}|$, where T is a test data set of about 5% randomly chosen reflections excluded from the refinement. Numbers in parentheses represent the value for the highest resolution shell.

Table S2. $C_{2\alpha}$ stereochemistry and relevant parameters in enzyme-free or enzyme-bound tetrahedral adducts with ThDP or 3-deaza ThDP.[a]

PDB ID[b]	Stereochemistry ($C_{2\alpha}$)	C_2–$C_{2\alpha}$ (Å)	$N_{4'}$–$C_{2\alpha}$ (Å)	$O_{2\alpha}$–$N_{4'}$(Å)	$O_{2\alpha}$–$C_{2\alpha}$–C_2 (°)	$O_{2\alpha}$–$C_{2\alpha}$–$C_{2\beta}$ (°)	C_2–$C_{2\alpha}$–$C_{2\beta}$ (°)
5EJ8 (MenD)	*S*	1.49	3.03	4.36	94.19	98.42	113.46
3DUF	*R*	1.53	3.32	2.30	109.81	111.15	109.04
2VBG	*R*	1.53	3.56	2.95	98.78	110.06	119.07
2Q5L[c]	*R*	1.54	3.37	2.60	110.98	112.43	110.84
2Q5L[c]	*S*	1.55	3.44	2.59	112.77	114.25	112.18
3ZHS	*S*	1.53	3.76	2.89	113.26	108.49	112.34
LIWREO	*S*	1.50	5.20	6.53	110.30	102.60	111.78
1GPU	---	1.27	2.95	2.96	132.79	119.46	107.75

5EJ8 (MenD)

Current work

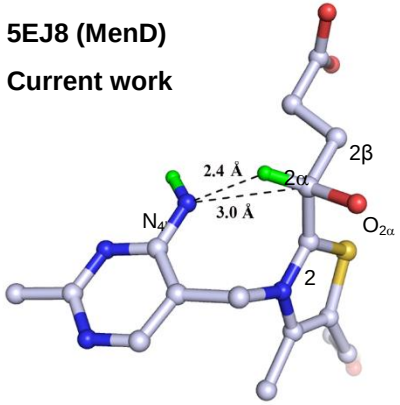

3ZHS

Succinic semialdehydre-ThDP

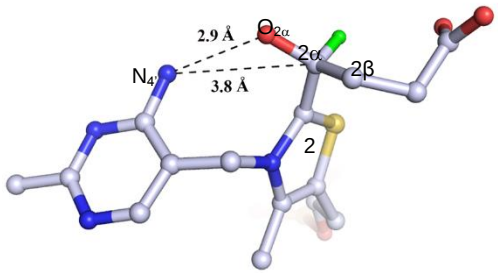

3DUF

2-(1-hydroxyethyl)-3-deaza-ThDP

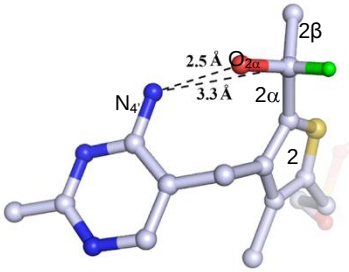

a. The adduct structures in 5EJ8 (Model II), 3ZHS and 3DUF are presented below the table with the N, H, O, S and C atoms in blue, green, red, gold and gray, respectively.

b. Only the ligand in one subunit (chain A) of the crystal structures is used; LIWREO is an enzyme-free ThDP adduct deposited in the Cambridge Crystallographic Data Centre (CCDC) (available at http://www.ccdc.cam.ac.uk/); An enamine intermediate from 1GPU is included for comparison.

c. Both conformations are modeled for 2-(1-hydroxyethyl)-3-deaza-ThDP in different subunits of 2Q5L.

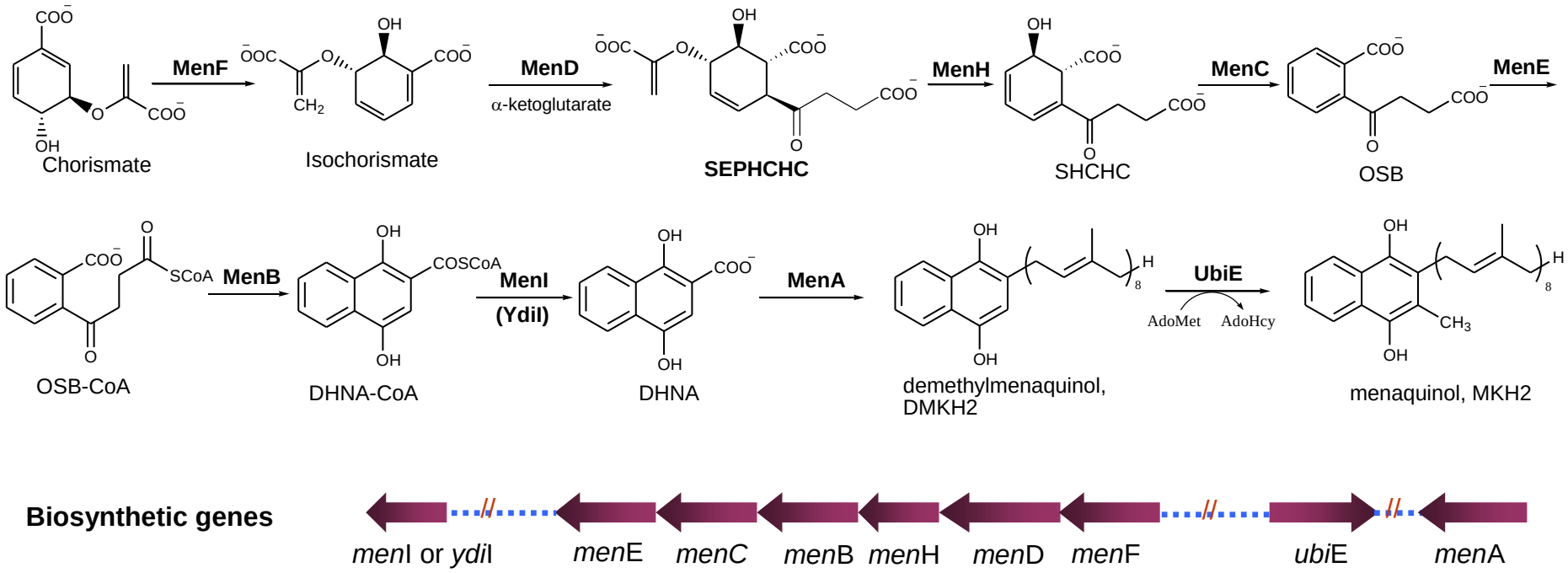

Figure S1. The biosynthesis of menaquinone (vitamin K2) in *Escherichia coli*. SHCHC: (1*R*, 6*R*)-2-succinyl-6-hydroxy-2, 4-cyclohexadiene-1-carboxylate; SEPHCHC:(1*R*, 2*S*, 5*S*, 6*S*)-2-succinyl-5-enolpyruvyl-6- hydroxy-3-cyclohexene-1-carboxylate; OSB: *o*-succinyl-1-benzoate; DHNA: 1, 4-dihydroxy-2-naphthanoate; CoA: coenzyme A; DMKH2: demethylmenaquinol; MKH2: menaquinol; AdoMet: *S*-adenosyl methionine; AdoHcy: *S*-adenosyl homocysteine.

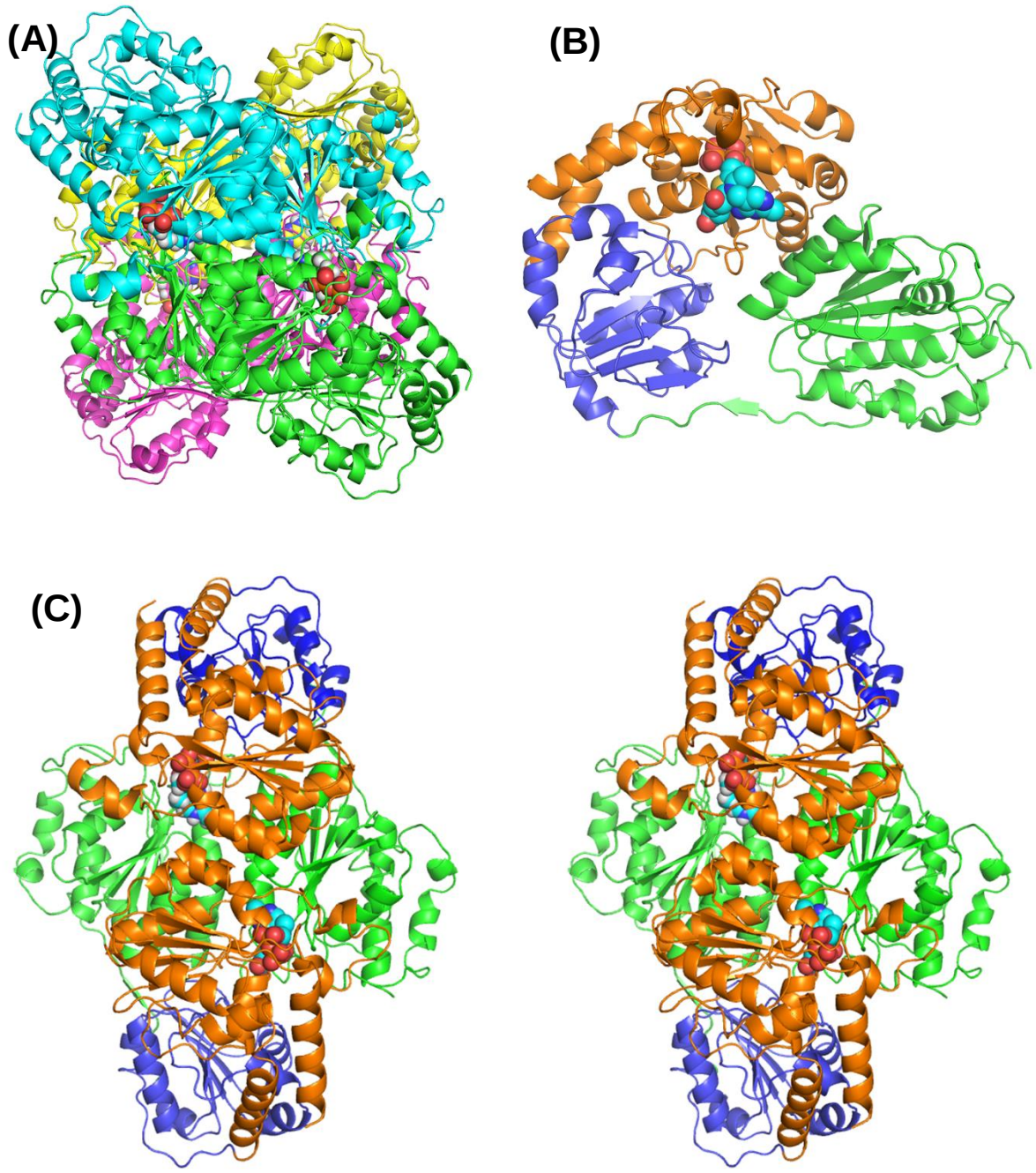

Figure S2. Crystal structure of *E. coli* MenD complexed with the tetrahedral intermediate. (**A**) The dimer-of-dimer assembly. (**B**) Domain structure of a MenD subunit. (**C**) Stereoview of an active dimer in the MenD structure. The structures are drawn from PDB ID 5EJ8 at 1.34 Å resolution and are colored by chains in (**A**) and by domains in (**B**) and (**C**). The tetrahedral intermediate is represented in spheres with carbon atoms colored in cyan.

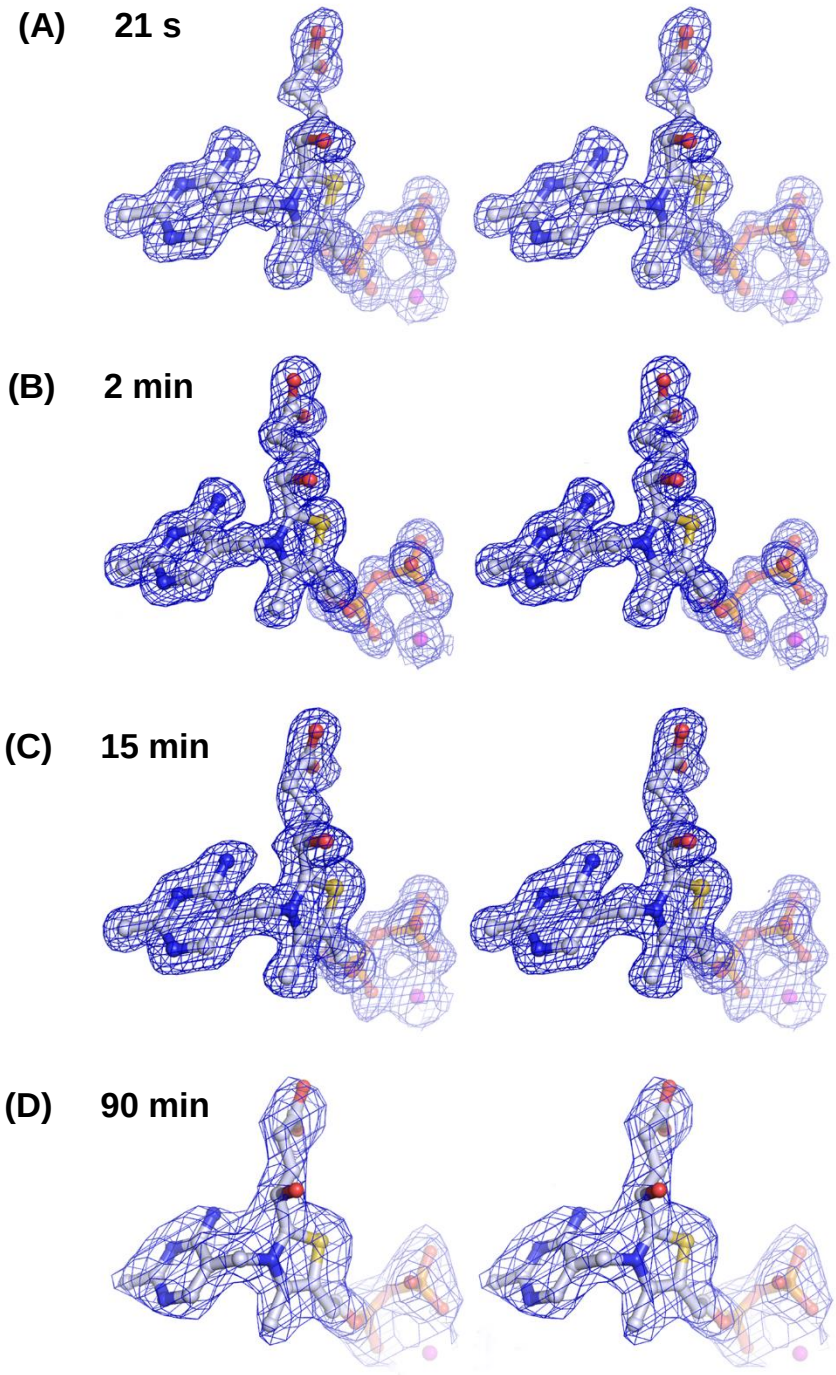

Figure S3. Stereo diagram of the 2mF_o-DF_c electron density map of the tetrahedral intermediate formed in MenD crystals after soaked with 10 mM α-ketoglutarate at room temperature for a varied time period: (**A**) 21s (PDB entry 5EJ7); (**B**) 2 min (PDB entry 5EJ8); (**C**) 15 min (PDB entry 5EJ4); and (**D**) 90 min (PDB entry 5EJ5). The maps are contoured at 1.0σ in blue mesh and (**B**) is the same as in Figure 2(**C**) except at a different contour level. The tetrahedral intermediate is represented in sticks with grey carbon atoms and the manganese (II) ion is denoted with a magenta sphere.

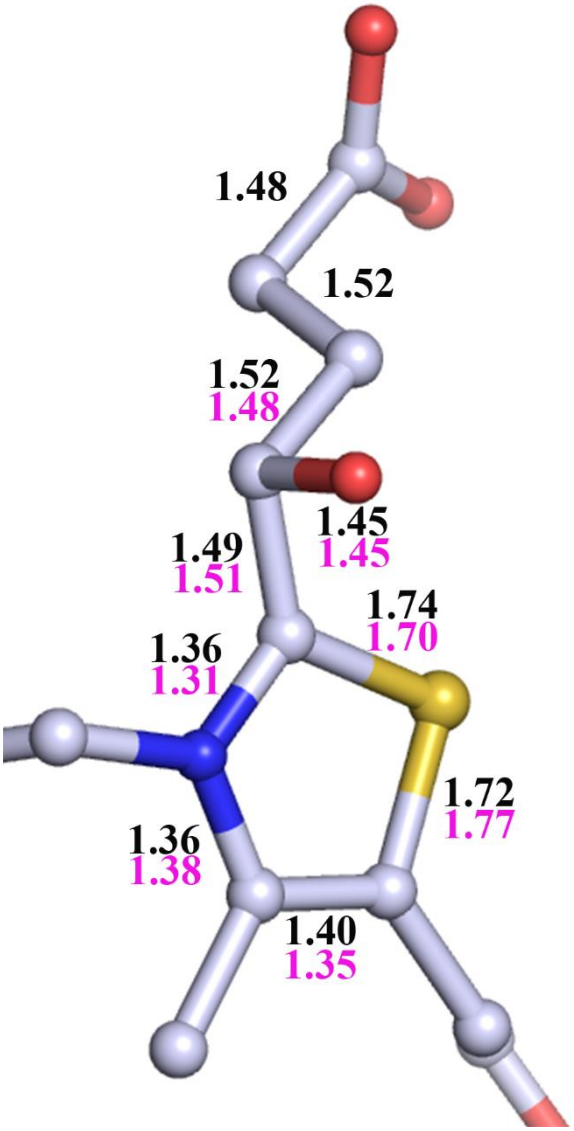

Figure S4. Lengths of chemical bonds in the thiazolium ring and the C_2-appendage in the MenD-bound postdecarboxylation intermediate compared to those in an enzyme-free 2-(1-hydroxyethyl)-ThDP.[18] The bond lengths are indicated in black for the MenD ligand and in pink for the enzyme-free molecule.

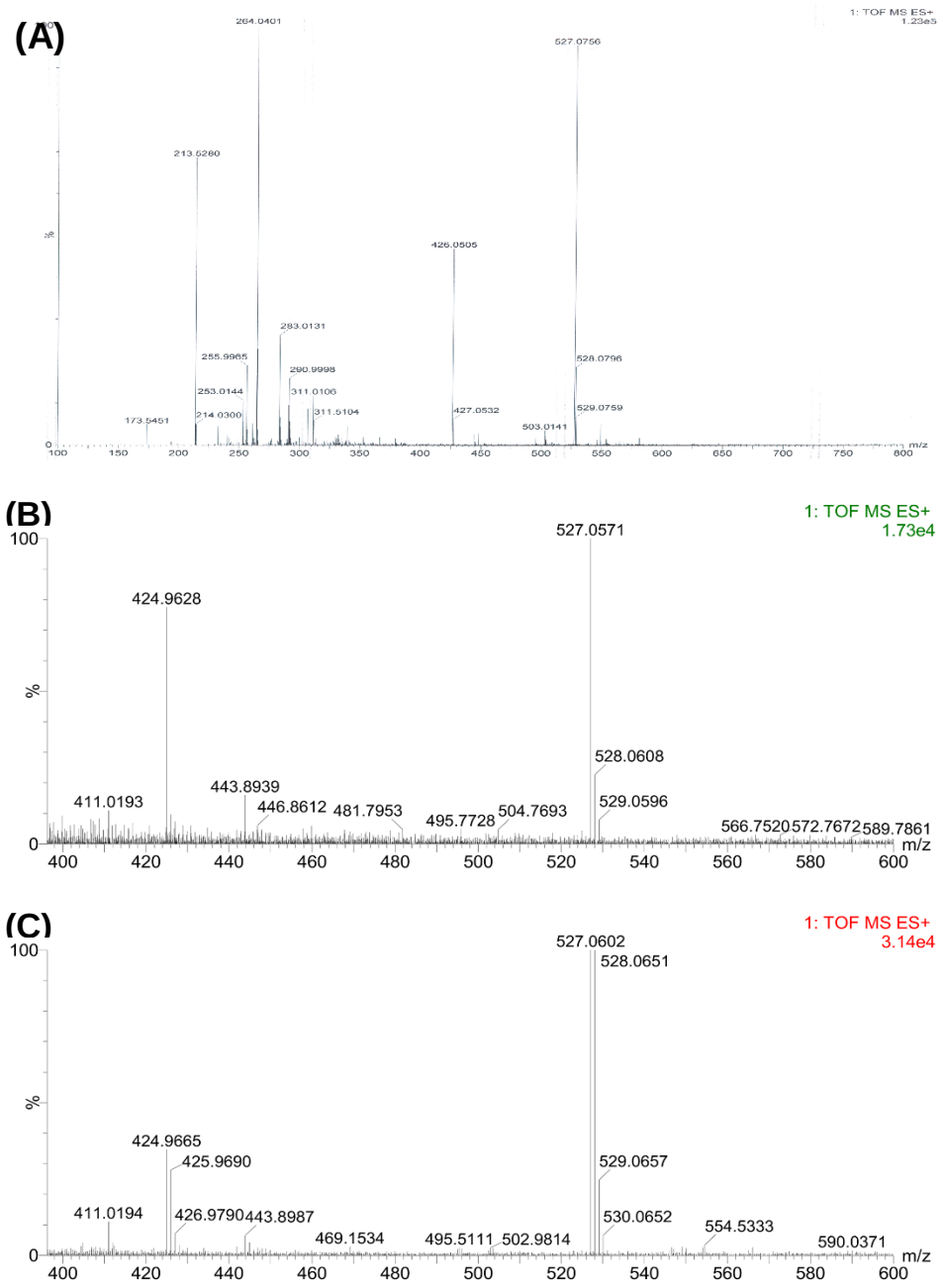

Figure S5. ESI-MS spectra of the products formed in the reaction between α-ketoglutarate and ThDP-bound MenD. (**A**) Product mixture from acid quenching of a normal reaction after 1 min. (**B**) ThDP adduct purified from the control reaction in the deuterium exchange experiment. (**C**) ThDP adduct isolated from the deuterium exchange reaction in the presence of 50% D_2O. Preparation and purification of the ThDP adduct in (**B**) and (**C**) are described in the Materials and Methods. Calculated exact molecular weights: ThDP ($C_{12}H_{19}N_4O_7P_2S^+$), 425.04; succinic semialdehyde-ThDP adduct ($C_{16}H_{25}N_4O_{10}P_2S^+$), 527.08; C2α-deuterated succinic semialdehyde-ThDP adduct ($C_{16}H_{24}DN_4O_{10}P_2S^+$), 528.08.

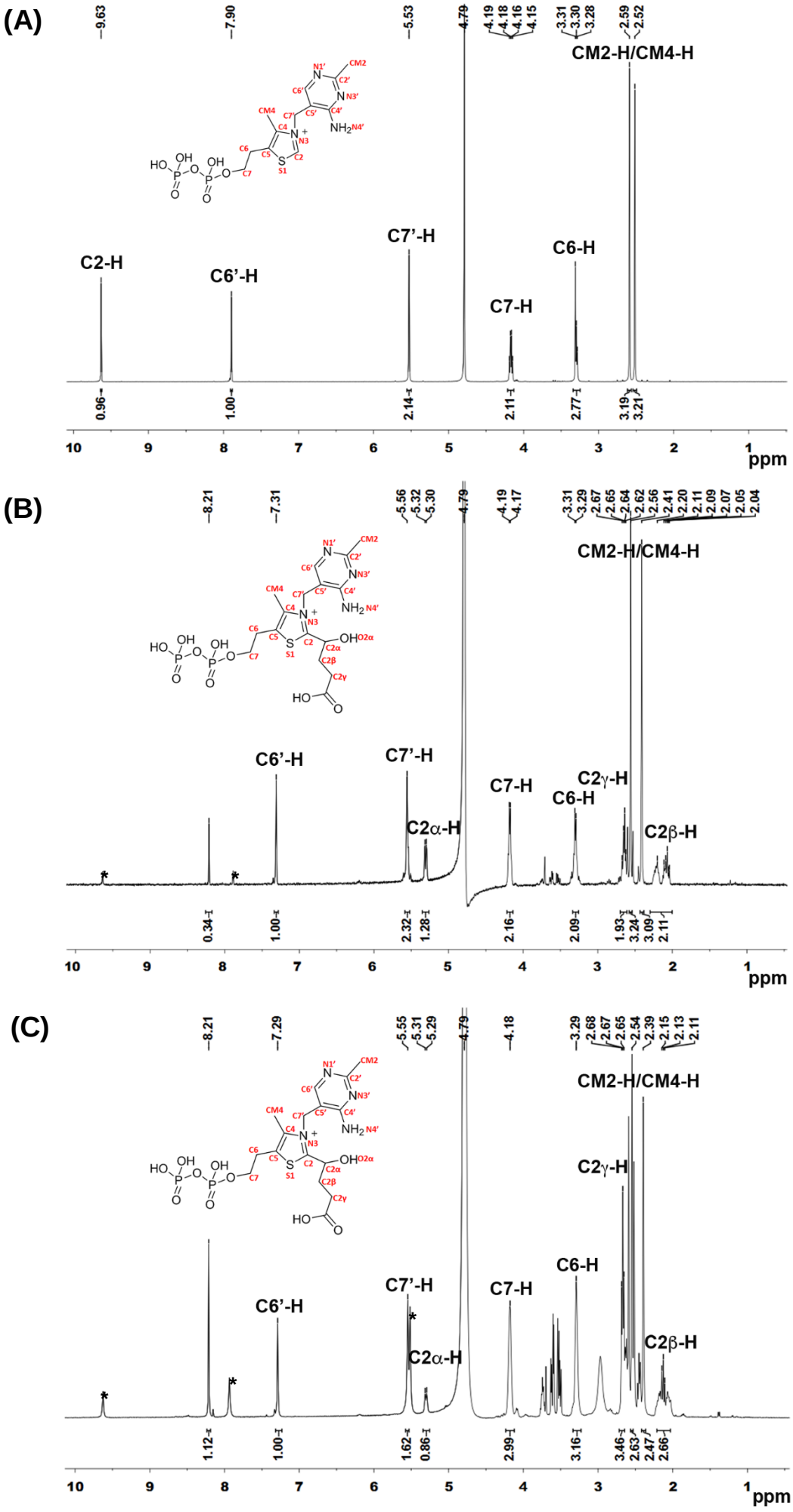

(See next page for the figure legend)

Figure S6. ^{1}H-NMR spectra of ThDP and the succinic semialdehyde-ThDP adduct from the deuterium exchange experiment. (**A**) ^{1}H-NMR spectrum of commercially available ThDP with signals properly assigned according to Spectral Database for Organic Compounds (SDBS) [National Institute of Advanced Industrial Science and Technology (AIST). ^{1}H-NMR spectrum; SDBS No.: 4986; HSP-41-999; http://sdbs.db.aist.go.jp (accessed Nov 26, 2015)]. (**B**) ^{1}H-NMR spectrum of the ThDP adduct purified from the control reaction in the deuterium exchange experiment. (**C**) ^{1}H-NMR spectrum of the ThDP isolated from the deuterium exchange reaction in the presence of 50% D_2O. All samples were dissolved in D_2O for the spectrum recording. The ThDP adduct in (**B**) and (**C**) was obtained and purified by HPLC from the deuterium exchange reactions described in the Materials and Methods. The $C_{6'}$-H signal at δ7.31 (**B**) or δ7.29 (**C**) was used as an internal standard to calculate the percentage of deuterium exchange at $C_{2\alpha}$-H due to its sensitivity to the identity of the covalent ThDP adduct .[19] Chemical shifts of $C_{6'}$-H, $C_{2\alpha}$-H and other protons were assigned by comparison to the ^{1}H-NMR signals of similar ThDP adducts reported earlier.[20-22] The peaks with an asterisk (*) are from free ThDP while the signal at δ8.21 is from an unknown impurity and the peaks at δ3.0 and δ3.50-3.75 are from glycerol in (**B**) and (**C**).

Supplementary References:

1. DeLano, W. L. The PyMOL Molecular Graphics System, DeLano Scientific, San Carlos, CA (2002).
2. Jiang, M.; Cao, Y.; Guo, Z. F.; Chen, M.; Chen, X.; Guo, Z. *Biochemistry* **2007**, *46*, 10979.
3. Liu, J.; Quinn, N.; Berchtold, G. A.; Walsh, C. T. *Biochemistry* **1990**, *29*, 1417.
4. Grisostomi, C.; Kast, P.; Pulido, R.; Huynh, J.; Hilvert, D. *Bioorg. Chem.* **1997**, *25*, 297.
5. Jiang, M.; Chen, X.; Guo, Z. F.; Cao, Y.; Chen, M.; Guo, Z. *Biochemistry* **2008**, *47*, 3426.
6. Sun, Y.; Yin, S.; Feng, Y.; Li, J.; Zhou, J.; Liu, C.; Zhu, G.; Guo, Z. *J. Biol. Chem.***2014**, *289*, 15867.
7. Otwinowski, Z.; Minor, W. *Method. Enzymol.***1997**, *276*, 307.
8. Battye, T. G. G.; Kontogiannis, L.; Johnson, O.; Powell, H. R.; Leslie, A. G. W. *Acta Crystallogr. Sect. D: Biol. Crystallogr.* **2011**, *67*, 271.
9. Evans, P. R.; Murshudov, G. N. *Acta Crystallogr Sect. D: Biol. Crystallogr.* **2013**, *69*, 1204.
10. Mccoy, A. J.; Grosse-Kunstleve, R. W.; Adams, P. D.; Winn, M. D.; Storoni, L. C.; Read, R. J. *J. Appl. Crystallogr.* **2007**,*40*, 658.
11. Dawson, A.; Fyfe, P. K.; Hunter, W. N. *J. Mol. Biol.* **2008**, *384*, 1353.
12. Emsley, P.; Lohkamp, B.; Scott, W. G.; Cowtan, K. *Acta Crystallogr. Sect. D: Biol. Crystallogr.* **2010**, *66*, 486.
13. Adams, P. D.; Afonine, P. V.; Bunkoczi, G.; Chen, V. B.; Davis, I. W.; Echols, N.; Headd, J. J.; Hung, L. W.; Kapral, G. J.; Grosse-Kunstleve, R. W.; McCoy, A. J.; Moriarty, N. W.; Oeffner, R.; Read, R. J.; Richardson, D. C.; Richardson, J. S.; Terwilliger, T. C.; Zwart, P. H. *Acta Crystallogr. Sect. D: Biol. Crystallogr.* **2010**, *66*, 213.
14. Schuttelkopf, A. W.; van Aalten, D. M.; *Acta Crystallogr. Sect. D: Biol. Crystallogr.* **2004**, *60*, 1355.
15. Moriarty, N. W.; Grosse-Kunstleve, R. W.; Adams, P. D. *Acta Crystallogr. Sect. D: Biol. Crystallogr.* **2009**, *65*, 1074.
16. Laskowski, R. A.; Macarthur, M. W.; Moss, D. S.; Thornton, J. M. *J. Appl. Crystallogr.* **1993**, *26*, 283.
17. Chen, V. B.; Arendall, W. B.; Headd, J. J.; Keedy, D. A.; Immormino, R. M.; Kapral, G. J.; Murray, L. W.; Richardson, J. S.; Richardson, D. C. *Acta Crystallogr. Sect. D: Biol. Crystallogr.* **2010**, *66*, 12.
18. Malandrinos, G.; Louloudi, M.; Mitsopoulou, C. A.; Butler, I. S.; Bau, R.; Hadjiliadis, N.; *J. Biol. Inorg. Chem.* **1998**, *3*, 437.
19. Tittmann, K.; Golbik, R.; Uhlemann, K.; Khailova, L.; Schneider, G.; Patel, M.; Jordan, F.; Chipman, D. M.; Duggleby, R. G.; Hubner, G. *Biochemistry* **2003**, *42*, 7885.
20. Lautens, J. C.; Kluger, R. *J. Org. Chem.* **1992**, *57*, 6410.
21. Balakrishnan, A.; Nemeria, N. S.; Chakraborty, S.; Kakalis, L.; Jordan, F. *J. Am. Chem. Soc.* **2012**, *134*, 18644.
22. Wille, G.; Meyer, D.; Steinmetz, A.; Hinze, E.; Golbik, R.; Tittmann, K. *Nat. Chem. Biol.* **2006**, *2*, 324.